Article citation info:
GE Z, WU F, YANG Y, LUO X. One cabin equipment location method based on the visibility human-factor potential field. Eksploatacja i Niezawodnosc – Maintenance and Reliability 2015; 17 (2): 236–242, http://dx.doi.org/10.17531/ein.2015.2.10.

Zhexue GE
Fuzhang WU
Yongmin YANG
Xu LUO

ONE CABIN EQUIPMENT LOCATION METHOD BASED ON THE VISIBILITY HUMAN-FACTOR POTENTIAL FIELD

METODA ROZMIESZCZANIA PRZYRZĄDÓW POKŁADOWYCH OPARTA NA POJĘCIACH POTENCJAŁOWEGO POLA WIDOCZNOŚCI ORAZ POTENCJAŁOWEGO POLA CZYNNIKA LUDZKIEGO

The visibility is the basic condition for cabin equipment location. For the description of human, object and obstacle, the human-factor potential field concept is proposed in this paper, concluding the visibility potential field, the reachability potential field. The cabin equipment layout problem is modeled based on the basic visibility potential field model. The optimal layout optimization method is studied based on the particle swarm optimization (PSO) algorithm by natural selection. Finally, the applicability of the proposed idea is illustrated by numerical studies.

Keywords: *cabin equipment, the human-factor potential field (HFPF), visibility potential field(VPF), layout optimization, particle swarm optimization (PSO).*

Widoczność jest podstawowym warunkiem przy projektowaniu rozmieszczenia przyrządów pokładowych. W przedstawionej pracy zaproponowano pojęcie potencjałowego pola czynnika ludzkiego (human-factor potential field, HFPF), które służy do opisu czynnika ludzkiego, przedmiotów oraz przeszkód. HFPF obejmuje pojęcia potencjałowego pola widoczności oraz potencjałowego pola dostępu. Problem umiejscowienia elementów wyposażenia kabiny zamodelowano na podstawie podstawowego modelu potencjałowego pola widoczności. Metodę optymalizacji rozmieszczenia elementów wyposażenia badano w oparciu o algorytm optymalizacji rojem cząstek (PSO), metodą naturalnej selekcji. Zastosowanie proponowanej koncepcji zilustrowano na przykładzie badań numerycznych.

Słowa kluczowe: *przyrządy pokładowe, potencjałowe pole czynnika ludzkiego (HFPF), potencjałowe pole widoczności (VPF), optymalizacja rozmieszczenia, optymalizacja rojem cząstek (PSO).*

1. Introduction

Ships, aircraft, armored vehicle, etc. usually consist of cabin structure, and there are a lot of cabin equipment requires manual inspection, monitoring, maintenance and operation [10]. In the cabin design process, visibility is one very important design factor to ensure the monitored equipment within the visual scope [9]. All the equipment to be maintained need reasonable operation space, and the determination of the space distribution of the equipment is an important part of the product design.

There are a large number of studies analyzing the visibility of product. However, in most cases the process is based on the graphics method and needs manual participation. Yin adopts visual cone method to assess the visibility of manufacturing process [12]. Bidault combines the method of clipping plane and visual cone [3]. In order to increase the design and analysis efficiency of the space layout design, the model based on visibility optimization design method is indispensable, but there are very few relative studies at present.

This paper mainly studies the cabin equipment layout method from the field point of view. To describe the relationship between the human body, the obstacle and the object, the conception of the human-factor potential field is put forward in the paper, and the mathematical model of visibility potential field is established. Then the optimization design method of space layout based on the visibility target is studied so as to improve the spatial layout of visual design efficiency and design quality. The layout optimization design model is established and solved by the particle swarm optimization algorithm.

2. The Human-factor Potential Field Concept

2.1. The artificial potential field

The artificial potential field (APF) method originated in the physics field theory [5, 7], which is first proposed by Khatbi in 1986 [7].It is artificially built similar to the physics potential field and can be applied to the study on some non-physics problems. The basic principle of APF can be summarized as follows. The motion of the manipulator or mobile robots can be considered in an abstract artificial force field. Target point X_{goal} generates attractive force on the robot X , and obstacle X_{obs} generates repulsion to the robot, and finally the motion of the robot is determined according to the composition of the forces. The direction of non-collision path is gotten by the direction of the descent potential function. The method has been widely used for real-time obstacle avoidance and smooth trajectory control.

Since the artificial potential field is one scalar field and its characteristics are similar to the electric field. The artificial potential field method creates a potential field U in the motion space of moving object. The potential field is composed of two parts: one is the attractive force field $\dot{U}_{att}$, it increases monotonically with the distance of the moving object and target, and directs to the target point; another is the repulsive force field $\dot{U}_{rep}$, it decreases monotonically with the increasing of moving object and obstacle distance and has a maximum value when the moving object in the location of obstacle. $\dot{U}_{rep}$ points to the direction opposite to the target point.

The total potential field is the sum of attractive force part and repulsive force part. The force of one moving object in the artificial potential field is the negative gradient of U:

$$F(X)=\dot{U}_{att}(X)+\dot{U}_{rep}(X)=-\nabla U(X) \tag{1}$$

The attractive force field in the whole area is defined as:

$$\dot{U}_{att}(X)=\frac{1}{2}\xi\rho^{m}\left(X,X_{goal}\right) \tag{2}$$

Where, ξ is the proportional coefficient, $\rho\left(X,X_{goal}\right)$ is the distance of moving object X to the object X_{goal}, $m=2$.

The attractive force of the moving object is the negative gradient of attractive potential energy:

$$F_{att}(X)=-\nabla U_{att}(X)=\xi\left(X,X_{goal}\right) \tag{3}$$

The force linearly goes to zero when the moving object approaches the target.

One general formula for the repulsive force field is:

$$\dot{U}_{rep}(X)=\begin{cases}\frac{1}{2}\eta\frac{1}{\rho\left(X,X_{goal}\right)}\cdots\rho\left(X,X_{obs}\right)\le\rho_0\\ 0\cdots\rho\left(X,X_{obs}\right)>\rho_0\end{cases} \tag{4}$$

The resultant of force is the composition of attraction and repulsion forces, i.e.:

$$F_{total}=F_{att}+F_{rep} \tag{5}$$

The next movement of the moving object can be determined by the force magnitude and direction.

2.2. The Human-factor Potential Field concept

Based on the definition of artificial potential field, the human-factor potential field (HFPF) is an artificial field to describe the impact of operator to the product. It reflects the interaction mechanism between operator and product operability features, and it includes the independent and complex field of human visibility, accessibility and comfort, potential field.

In the HFPF, each design unit structure will have some human-factor potential energy, the body and optimal human performance region produce attractive force to the unit, while the repulsion forces are produced between the different structures. Thus the dynamic change of the product structure and layout can be driven, and the best location for the design unit can be found to maximize the attractive force.

Definition 1: The HFPF refers to the artificial field interaction between various human factors and environment subjects. It can be formulated as (6):

$$U(X)=u(h_i(X),e_j(X)) \tag{6}$$

Where, $h_i(X)$ is the human factor parameter of space point $X=(x,y,z)$, and $e_j(X)$ is the environmental parameter of X. According to the artificial potential concept, the HFPF can be divided into the gravitational potential field U_{att} and the repulsive potential field U_{rep}, and the former is produced by the target and operator, while the latter is produced by the interactions of obstacles and operator.

The human-factor ability includes a lot of factors. Visual, auditory, tactile, olfactory, proprioceptive, etc. are associated with the feeling, and working space, comfort, etc. are associated with exercise capacity. So the HFPF includes visibility potential field, auditory potential field, tactile potential field, olfactory potential field, accessibility and other potential field, etc. This paper mainly focuses on the visibility potential field.

Definition 2: The visibility potential field $U_C(X)$ describes the interaction of eyes and all space points. It represents the space observation ability of eyes and can be formulated as (7):

$$U_C(X)=u_c(h_{ci}(X),e_{cj}(X)) \tag{7}$$

Where, $h_{ci}(X)$ represents the parameters associated with visibility, such as visual acuity, visual field, visual range and visual fatigue [1, 2, 4, 8, 11]. $e_{ci}(X)$ represents the environment parameters associated with visibility, such as light environment, obstacles between the target point and the human eye.

3. The modeling of visibility potential field

3.1. The visibility potential model

The visibility potential field (VPF) can be expressed as the sum of the attractive filed function and repulsion field function as follows:

$$U_C(X_P)=U_{C\_att}(X_P)+U_{C\_rep}(X_P) \tag{8}$$

Where, $U_{C\_att}(X_P)$ is the attractive visibility potential field. The influence factor of the eye enginery includes the amount of visual field, the visual distance and so on. The influence factor of the environment concludes obstacle, light and so on[9]. For simplicity, the visual field and visual distance are to be considered in the paper.

$$U_{C\_att}(X_P)=u\left(C_\theta(X_P),C_l(X_P),C_{light}(X_P)\right)=1-C_\theta(X_P)\bullet C_l(X_P) \tag{9}$$

Where, $C_\theta(X_P)$, $C_l(X_P)$ are the eye visual function. They can denote the relationship of visibility with the visual field and visual distance respectively. $X_P=\{x_P,y_P,z_P\}$ is the coordinate of the point P.

$U_{C\_rep}(X_P)$ is the repulsion visibility potential field. It can be expressed as follows:

$$\begin{aligned}U_{C\_rep}(X_P)&=U\left(C_e(X_P),C_\theta(X_P),C_l(X_P),C_{obs}(X_P)\right)\\&=C_e(X_P)\bullet C_\theta(X_P)\bullet C_l(X_P)\bullet C_{obs}(X_P)\end{aligned} \tag{10}$$

Then ,the visibility potential energy function is formula (11):

$$\begin{aligned} U_C(X_P) &= U_{C\_cat}(X_P) + U_{C\_rep}(X_P) \\ &= 1 - C_e(X_Q) \bullet C_\theta(X_Q) \bullet C_l(X_Q) \bullet (1 - C_{obs}(X_P)) \end{aligned} \tag{11}$$

Where $C_{obs}(X_P)$ represents the effect function of the obstacle to visibility.

3.2. The visual field function

The visual field is the space that can be seen by eyes when the environment and head remain stationary. According to the relationship between visual field and visibility in literature 5, visual field function is defined as follows:

$$C_\theta(X) = C_{\theta y}(X) \bullet C_{\theta x}(X) \tag{12}$$

When the head remained stationary but eye in the rotation, vertical field of human normal sight direction is horizontal line of 15 degree down, which is the human natural angle of sight. The line of sight of the upper and lower 15° is the comfortable vertical visual field, and the maximum vertical field of view is the region of above the normal sight line of sight 40° to 20° below [9]. Some representative point values of vertical visual field can be gotten as Table 1.

Table 1. Some representative direction values of vertical visual field

Direction number	Angle (degree)	Visibility value
1	-20	0
2	-15	0.8
3	0	1
4	15	0.8
5	40	0

Based on Table 1, the relationship between $C_{\theta y}$ and vertical sight angles can be gotten by polynomial fitting. It can be formulated as follows:

$$C_{\theta y} = 2.8120\theta_y{}^3 - 4.9801\theta_y{}^2 + 0.5892\theta_y + 1.0495 \tag{13}$$

Similarly, the scope between 15° left and right of the center line is the best horizontal vision scope of both eyes, while the scope between 13° left and right of the center line is the maximum field of view. Some representative point values of horizontal visual field can be gotten as Table 2.

Table 2. Some representative direction values of horizontalvisual field

Direction number	Angle (degree)	Visibility value
1	-35	0
2	-15	0.8
3	0	1
4	15	0.8
5	35	0

The horizontal visual field C_{θ_x} can be formulated as(14):

$$C_{\theta x} = -0.2089\theta_x{}^3 - 2.7580\theta_x{}^2 + 0.1103\theta_x + 1.0596 \tag{14}$$

Where θ_x is the horizontal visual angle of sight.

3.3. Visual distance function

The visual distance in operation directly affects the reading speed and accuracy, it should be determined by the size and shape of observation object. Usually, the most suitable visual region is 38~76 cm, less than 38 cm can cause dizziness, more than 76 cm may lose details. Using 4 order polynomial fitting, visibility distance function ξ_j can be gotten as:

$$C_l = 9.9531\times10^{-8} \bullet l^4 - 2.0927\times10^{-5} \bullet l^3 + 0.0011\times10^{-2} \bullet l^2 - 2.7047\times10^{-4} \bullet l + 0.0038 \tag{15}$$

Where, n is the visual distance.

3.4. Obstacle influence function

Among the environmental factors, the impact of obstacles is mostly concerned. When people are watching the object, the obstacle blocked area cannot be seen. The obstacle influence function should be formulated according to the geometric relations of human, obstacle and space point. Suppose the eye locates at point O, and the obstacle locates at point O', the obstacle is simplified to a circular area of radius R_{obs}. $\overrightarrow{l_{\mathrm{obs}}} = \overrightarrow{OO'}$ is the distance between the obstacle and eye, θ_{R} is angel between obstacle edge and eyesight baseline. For space point P, the distance to eye is (x_i, y_i). Then the obstacle visibility function C_{obs} can be expressed as follows:

$$C_{obs} = \begin{cases} 0 & if \ \left|\overrightarrow{l_P}\right| > \left|\overrightarrow{l_{obs}}\right| \text{ and } \theta_{\mathrm{P}} \le \theta_{\mathrm{R}} \\ 1 & if \ \left|\overrightarrow{l_P}\right| > \left|\overrightarrow{l_{obs}}\right| \text{ and } \theta_{\mathrm{P}} > \theta_{\mathrm{R}} \\ 1 & if \ \left|\overrightarrow{l_P}\right| \le \left|\overrightarrow{l_{obs}}\right| \end{cases} \tag{16}$$

In order to ensure C_{obs} can be continuous and differentiable, the obstacle surrounding area is looked as the transition region. Suppose C_{obs} changes from 1to 0 between θ_{R} and θ_M. Then C_{obs} can be smoothed as formula (17).

$$C_{obs} = \begin{cases} 0 & \text{if } \left|\overrightarrow{l_P}\right| > \left|\overrightarrow{l_{obs}}\right| \text{ and } \theta_{\mathrm{P}} \le \theta_{\mathrm{R}} \\ a \bullet \left(\theta_P - \theta_R\right)^3 + b \bullet \left(\theta_P - \theta_R\right)^2 + c \bullet \left(\theta_P - \theta_R\right)^3 + d & \text{if } \left|\overrightarrow{l_P}\right| > \left|\overrightarrow{l_{obs}}\right| \text{ and } \theta_{\mathrm{R}} < \theta_{\mathrm{P}} \le \theta_{\mathrm{M}} \\ 1 & \text{if } \left|\overrightarrow{l_P}\right| > \left|\overrightarrow{l_{obs}}\right| \text{ and } \theta_{\mathrm{P}} > \theta_{\mathrm{M}} \\ 1 & \text{if } \left|\overrightarrow{l_P}\right| \le \left|\overrightarrow{l_{obs}}\right| \end{cases} \tag{17}$$

Where:

$$a = -1 \Big/ (\theta_M^3 - \theta_R^3 - 3\theta_R^2\theta_M^3 + 3\theta_R^4 - 3\theta_M^4\theta_R + 3\theta_M\theta_R^3 - 3\theta_M^5 + 3\theta_M^2\theta_R^2)$$

$$b = 3(-\theta_M^3 + \theta_R^2) \Big/ (-\theta_M + \theta_R)(\theta_M^3 - \theta_R^3 - 3\theta_R^2\theta_M^3 + 3\theta_R^4 - 3\theta_M^4\theta_R + 3\theta_M\theta_R^3 - 3\theta_M^5 + 3\theta_M^2\theta_R^2)$$

$$c = -\frac{-3\theta_M\theta_R(\theta_M - \theta_R^2)}{(-\theta_M + \theta_R)(\theta_M^3 - \theta_R^3 - 3\theta_R^2\theta_M^3 + 3\theta_R^4 - 3\theta_M^4\theta_R + 3\theta_M\theta_R^3 - 3\theta_M^5 + 3\theta_M^2\theta_R^2)}$$

$$d = -\frac{-\theta_M(3\theta_R^3 - 6\theta_M^2\theta_R^2 - \theta_M^3 + 3\theta_M^5 - \theta_R\theta_M^2)}{(-\theta_M + \theta_R)(\theta_M^3 - \theta_R^3 - 3\theta_R^2\theta_M^3 + 3\theta_R^4 - 3\theta_M^4\theta_R + 3\theta_M\theta_R^3 - 3\theta_M^5 + 3\theta_M^2\theta_R^2)}$$

Using MATLAB software, the space distribution of VPF can be drawn based on the VPF model. Different color can demonstrate the potential difference of every space point in the three-dimension map.

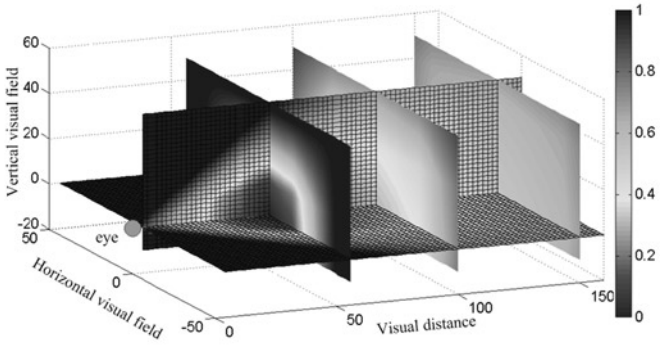

Fig. 1. Distribution of VPF without obstacle

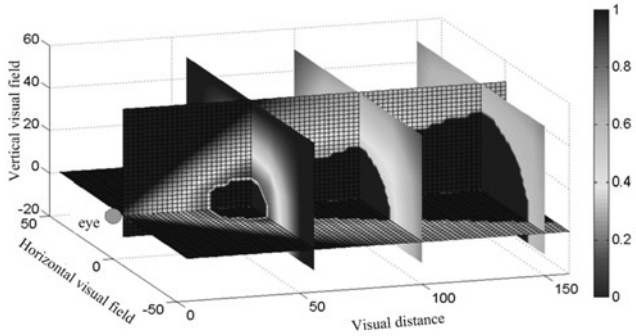

Fig. 2. Distribution of VPF with obstacle

Choose $\theta_M = 1.1\theta_R$. The lower potential ,the better visibility. The cross section perpendicular to the eyesight line can reflect the VPF of certain visual distance. Fig. 1. shows the VPF when the distance is 56 cm. When an obstacle exits at (0,0,50) with a radius of 10 cm, the VPF can be shown as Fig. 2., from which we can see that the VPF of blocked area is or close to 1, which means very poor visibility.

4. Space visibility optimizing layout

4.1. Modeling

Layout optimization modeling includes the determination of the optimization variables, objective function and the constraints.

(1) Objective function

It can be approximated considered that the visibility potential energy of one equipment is the sum of all the face points. Since not every point on the equipment has visibility requirement, the visibility potential energy can mainly concentrate on the highly required points that is the critical visual point. Then, the i-th object visibility function can be $U_C(i)=\sum_{j=1}^{m}\xi_{ij}U_C(X_{ij})$, where, m is the number of critical visual points on the target, ξ_{ij} represents the weight of the j-th key visual point, $0 \le \xi_{ij} \le 1$, and $\sum_{j=1}^{m}\xi_{ij}=1$. U_j represents the visibility potential energy of j -th critical visual point.

The comprehensive visibility potential energy represents the visibility of space layout design, which is the weighted sums of the visibility of all objects in the layout space, as $U_C=\sum_{i=1}^{n}\psi_i \bullet U_C(i)$, where, n expresses the number of layout objects, ψ_i is the weight of i-th object, $0 \le \psi_j \le 1$, and $\sum_{i=1}^{n}\psi_j=1$, $U_C(i)$ specifies the visibility potential energy of i-th object.

Therefore, the objective function can be expressed as follows:

$$\begin{cases} \max U_{com} = \max \sum_{i=1}^{n}\psi_i \sum_{j=1}^{m}\xi_{i,j} \bullet U_{i,j} \\ 0 \le \psi_i \le 1, 0 \le \xi_{i,j} \le 1, \sum_{i=1}^{n}\psi_i = 1, \sum_{j=1}^{m}\xi_{i,j} = 1 \end{cases} \tag{18}$$

(2) Representation of geometric objects

In this paper 2D plane layout problem is studied. Layout objects are simplified as rectangles or circles. The center coordinates (x_i, y_i), length l_i and width b_i size of rectangle is used to express geometric information of objects. The center coordinates (x_i, y_i) and radius R_i of rectangle are used to express geometric information of objects, which are showed in the Fig. 3.

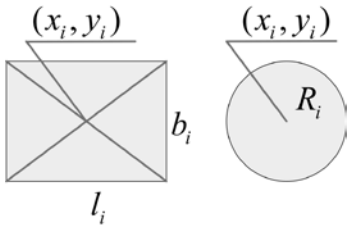

Fig. 3. Geometric information of object

(3) Constraint conditions

Constraint conditions mainly include the geometric constraint. Geometric constraint contains non-interference and boundary conditions. Non-interference conditions require that there is no overlapping part. Boundary conditions require that any object cannot beyond the given layout space.

The constraint conditions is defined as follows:

$$s.t. \begin{cases} g_i(x) > 0 \\ h_i(x) = 0 \end{cases} \tag{19}$$

Where, $g_i(x) > 0$ and $h_i(x) = 0$ respectively represent the inequalities and ebullition of the constraint conditions.

4.2. Algorithm of layout optimization

The model solution belongs to a NP problem, which could be solved by genetic algorithm, simulated annealing algorithm and particle swarm optimization. In this paper, the particle swarm optimization with advantage of simple structure and fast convergence speed has been adopted. The flow chart of layout optimization algorithm is shown in Fig. 4.

The first step is importing the information of layout. The second step is modeling the layout optimization. The third step is solving the layout optimization model. The last step is outputting the result of layout optimization [6]. Parameter setting includes the size, the number of key point and visibility weight of the objects. The position and speed updating method is defined as follows:

$$\begin{aligned} \mathrm{v}_{i,j}(t+1) &= w\mathrm{v}_{i,j}(t) + c_1 r_1[p_{i,j} - \mathrm{x}_{i,j}(t)] + c_2 r_2[p_{i,j} - \mathrm{x}_{i,j}(t)] \\ \mathrm{x}_{i,j}(t+1) &= \mathrm{x}_{i,j}(t) + \mathrm{v}_{i,j}(t+1), j = 1,2,\ldots,d \end{aligned} \tag{20}$$

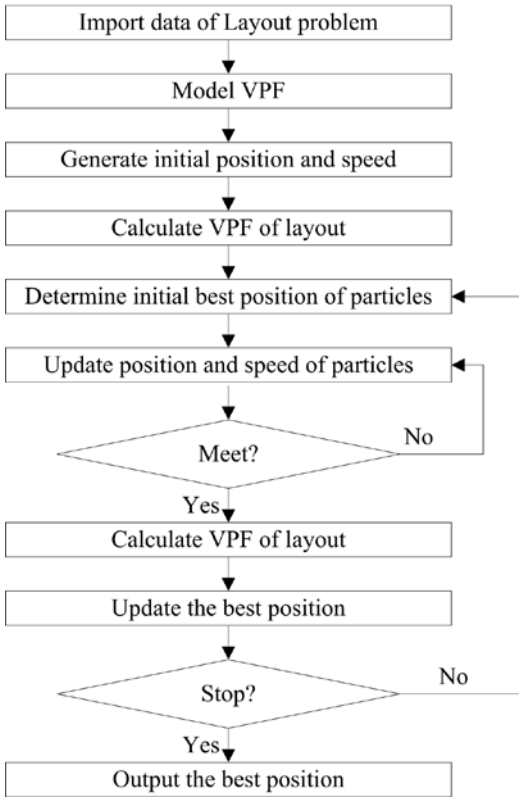

Fig. 4. Particle swarm optimization of layout optimization

Where, x and v respectively represent the position and speed of particles. c_1 and c_2 represent the learning factor. r_1 and r_2 represent the random numbers.

When updating the best particle position and speed, the particle swarm is sorted by the fitness value, the position and speed of the half of the poorest particles are replaced by half of the best particles. The stopping criterion is the iterative times and iterative accuracy.

5. Example and analysis

5.1. Problem Description

Assuming a certain type of cabin is circular with a radius of 50cm, there is a fixed internal obstacle. Within the spare space, the equipment (named A, B, C, D) layout problem is to be considered. The position to be monitored is at each geometric center of the equipment. The operator is parallel to the cabin plane with a distance of 60 cm, and the eyesight is perpendicular to the cabin plane. Between the operator and the cabin there is a circular visual obstacle, with a radius of 10 cm, and the distance from the cabin floor is 40 cm. The position relationship between each other is shown in Fig. 5. For simplicity, assume the body posture and eyesight are fixed. The initial layout is shown in Fig. 6. The size, initial position and weight of the key viewpoint are shown in Table 1.

Table 1. Parameters of object

Serial number	Length l_i(cm)	Width b_i(cm)	Initial Position
1	30	20	(0, 30)
2	R_2=10		(35, 0)
3	20	20	(0, −25)
4	16	16	(−20, 3)

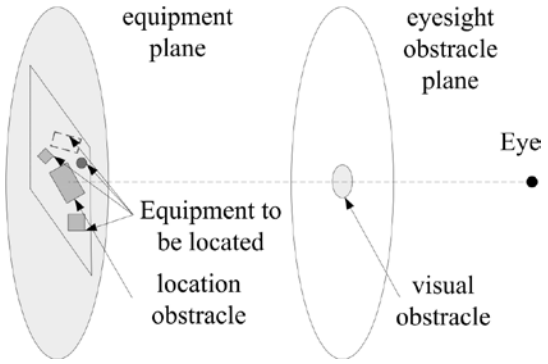

Fig. 5. The relationship of the equipment to be optimized

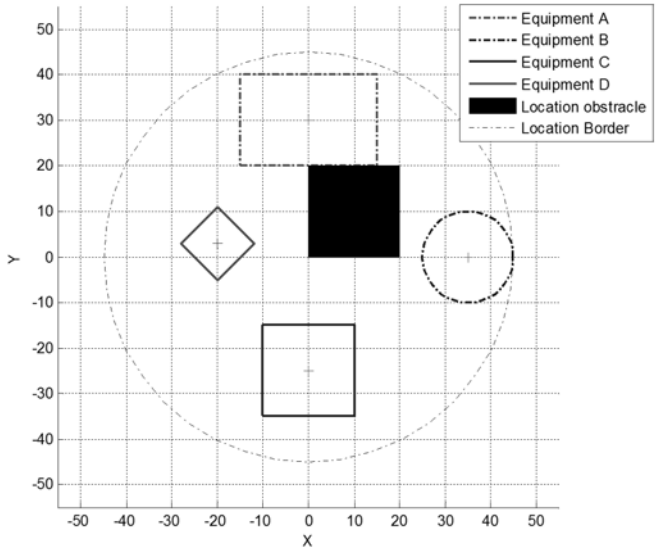

Fig. 6. Initial Position of all objects

The layout of the equipment must meet that there is no collision between each equipment and the barrier, and the visibility of the monitor points is the best. The HFPF method is applied for the optimal solution. It can be calculated that the VPF of the initial layout is 1.1348.

5.2. Modeling

According to the visibility model, the objective function is established as follows:

$$\min U_C = \min \sum_{i=1}^{4} c_i \bullet U_{Ci}$$

The constraint condition is determined as follows:

(1) Non-interference condition is determined as $\left|x_i - x_j\right| > \frac{l_i + l_j}{2}$

or $\left|y_i - y_j\right| > \frac{b_i + b_j}{2}$ $i = A,B,C,D,E$; $j = A,B,C,D,E$

(2) Boundary Conditions:
Boundary conditions are determined as follows:

$$\sqrt{x_i^2 + y_i^2} + \sqrt{l_i^2 + b_i^2}\,/2 < R \text{ (Rectangular)} \quad \sqrt{x_i^2 + y_i^2} + R_i < R \text{ (Circle)}$$

5.3. Simulation results and analysis

The MATLAB software is used to obtain the layout designed scheme with the best VPF index. Particle number, learning factor and the iterative times are respectively set at 40, 2 and 1000. Let $\theta_M = 1.1\theta_R$ in formula (17). Inertia weight uses adaptive weight method and the nonlinear dynamic inertia weight.

(1) When no visual obstacle exits, the layout result based on the particle swarm optimization method is showed in Fig. 7. Compared with the VPF of initial layout, the VPF of layout reduces greatly to 0.2452.

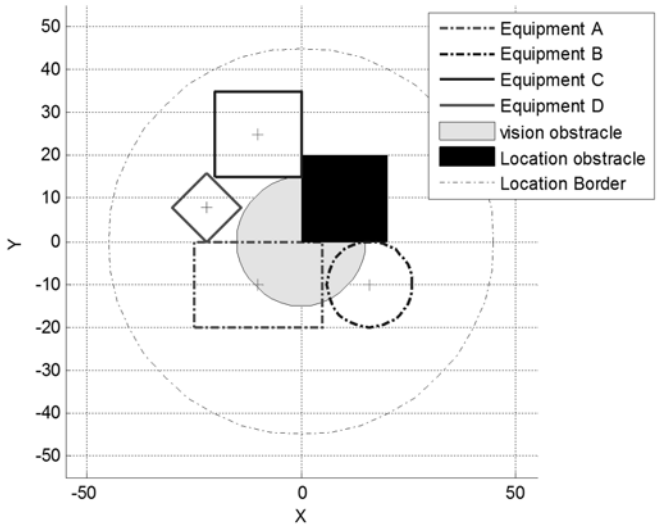

Fig. 7. The result of layout optimization without obstacles

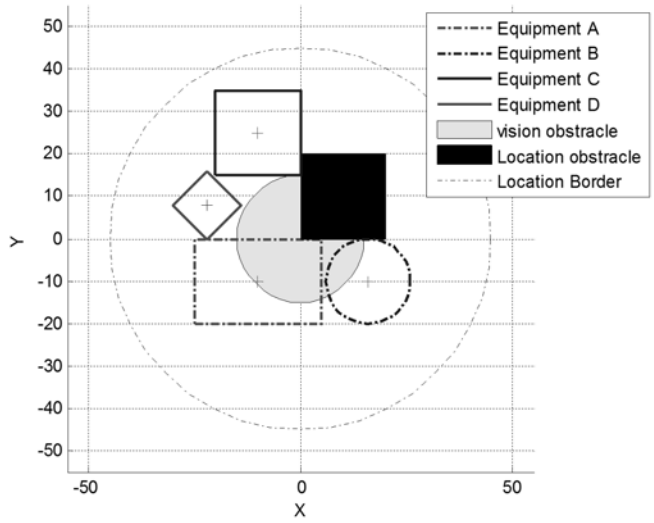

Fig. 8. The result of layout optimization with the obstacles

(2) When the visual obstacle located at point (0,0,60), the layout optimization result is shown in Fig.8. The VPF of layout is 0.4124, we can see that all the key visual points of objects can avoid the invisible area caused by the visual obstacle.

(3) The convergence speed of fitness value is shown in Figure 9. The VPF reaches 0.2452and become stable while iterative times are 252. It can also be demonstrated that PSO method with adaptive weight has strong convergence ability, which not only can avoid finding the local optimal value, but also has very fast convergence speed.

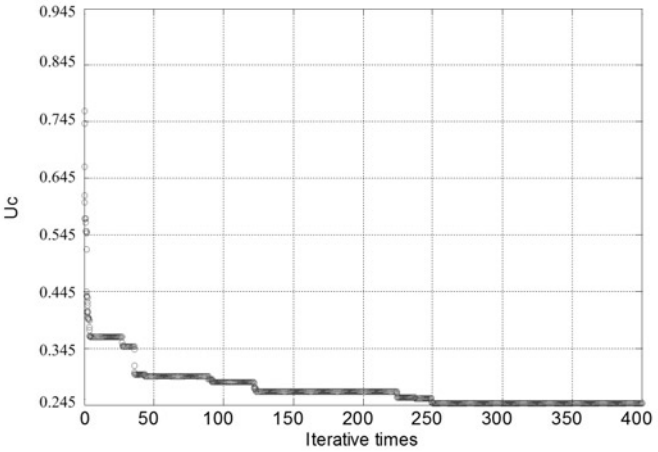

Fig. 9. Convergence speed of PSO

6. Conclusion

The human-factor potential field concept is proposed based on the traditional artificial field, concluding the visibility potential field, the reachability potential field and so on. It can describe the relationship of human, object and obstacle. The basic visibility potential field model is composed of vertical visual field, horizontal visual field, obstacle influence and so on. In order to realize optimization of visibility, the layout optimization method based on the VPF is put forward. The particle swarm optimization based method on natural selection is applied to solve the model, which can obtain the optimal solution with faster convergence speed. However only the plane layout is concerned in this paper, the complex three-dimensional layout should be studied in the future.

Acknowledgement

The research work is financed by the project of National Natural Science Foundation of China 51005238.

References

1. Abdel-Malek K, Yang J, Brand R, Tanbour E. Towards understanding the workspace of the upper extremities. SAE Transactions Journal of Passenger Cars: Mechanical Systems 2001; 6: 2198-2206.
2. Bendsoe MP, Sigmund O. Topology Optimization: theory, methods and applications. NewYork: Springer-Verlag Berlin Heidelberg 2003: 35-55.
3. Bidault F, Chablat D, Chedmail P, Pino L. A distributed approach for access and visibility task with a manikin and a robot in a virtual reality environment. IEEE Transactions on Industrial Electronics2003; 4: 692-698.

4. Blackmore D, Samulyak R, Leu MC. A singularity theory approach to swept volumes. International Journal of Shape Modeling 2000; 6: 105-129, http://dx.doi.org/10.1142/S0218654300000089.
5. Gilbert EG, Johnson D W. Distance functions and their application to robot path planning in the presence of obstacles. IEEE J Robotics and Automation 1985; 1: 21-30, http://dx.doi.org/10.1109/JRA.1985.1087003.
6. Ji Z; Liao HL, Wu QH. Particle swarm algorithm and its application. Beijing: Science Press; 2008.
7. Khatib O. Real-time obstacle avoidance for manipulators and mobile Robots[J]. The International Journal of Robotics Research 1986; 1:90-98, http://dx.doi.org/10.1177/027836498600500106.
8. Liu JL, Zen F M, Su QJ. Study on application of ergonomics based on CATIA in virtual design of marine power plant [J]. Journal of Wuhan university of technology social sciences edition 2008; 4: 657-660.
9. Sun YL. Human factors engineering [M]. Beijing: Science and Technology of China Publishing House; 2005.
10. Tjiparuro Z, Thompson G. Review of maintainability design principles and their application to conceptual design. Proceedings of the Institution of Mechanical Engineers, Part E: Journal of Process Mechanical Engineering 2004; 2:103-113, http://dx.doi.org/10.1243/095440804774134280.
11. Yang JZ, Sinokrot T, Abdel-Malek K. A general analytic approach for SantosTM upper extremity workspace. Computers & Industrial Engineering 2008; 54: 242-258, http://dx.doi.org/10.1016/j.cie.2007.07.008.
12. Yin ZP, Ding H, Xiong YL. Visibility theory and algorithms with application to manufacturing processes. International Journal of Production Research 2000; 13:2891-2909, http://dx.doi.org/10.1080/00207540050117350.

Zhexue GE
Laboratory of Science and Technology on Integrated Logistics Support
School of Mechatronics Engineering and Automation
National University of Defense Technology
De Ya Road, 109, Changsha, Hunan 410073, P. R. China

Fuzhang WU
China Aerodynamics Research and Development Center
Mian yang, Sichuan 621000, P. R. China

Yongmin YANG
Xu LUO
Laboratory of Science and Technology on Integrated Logistics Support
School of Mechatronics Engineering and Automation
National University of Defense Technology
De Ya Road, 109, Changsha, Hunan 410073, P. R. China

E-mails: gzx@nudt.edu.cn, lsai@cardc.cn, yangyongmin@163.com